

Supplementary Information for A Comparative Techno-Economic Analysis of Renewable Hydrogen Production Using Solar Energy

Methods

Photoelectrochemical Systems Costs

Window Considerations

Poly(methyl methacrylate (Plexiglass®), as has been used in previous studies, was not recommended by an industry supplier, based on chemical compatibility with the operating conditions of this design.^{1,2} Systems operating in alkaline media will require an alternative to glass (unstable), such as an ethylene tetrafluoroethylene (ETFE, Fluon® from Asahi Glass)-coated glass or another alkaline-stable material that is transparent to solar illumination; this requirement would likely increase the window component cost.

PEC Membrane Considerations

A density of $2 \text{ g} \cdot \text{cm}^{-3}$ (based on acid functionalized membranes³), a thickness of 5 mil (~127 microns) and a cost of \$2000/kg was used to calculate the \$ - m^{-2} PEC for Nafion based on a Nafion area requirement of 10% of the PEC area.

Type 4 PEC Concentrating Optics Considerations

A variety of concentrating optics can provide non- or minimal tracking 10x light concentration: compound parabolic concentrators (CPC), Fresnel lenses, dielectric totally internally reflecting concentrators (DTIRC) and prismatic concentrators.⁴ Commercial availability of low-concentrating optics for solar applications is limited to two-dimensional compound parabolic troughs, prismatic concentrators and, on small-scale, three-dimensional parabolic concentrators. Concentrator areal costs could only be obtained for CPCs, and the two-dimensional trough architecture provided the lowest costs, \$48 m^{-2} .^{1,5} A relatively low volume (highest volume quote available) quote for three-dimensional compound parabolic concentrators (13x concentration ratio) of $\$1.9 \times 10^5 \text{ m}^{-2}$, which is four orders of magnitude larger than the two-dimensional analog used in the study.

PV-E Sizing

The photovoltaic electrolysis system was sized such that the photovoltaic array would produce the exact amount of energy needed to produce the desired hydrogen output, 10,000 kg/day, and the electrolysis units were sized to accept the maximum instantaneous power output by the photovoltaics, assumed to be $1000 W_p m^{-2}$. For the base-case economics, this arrangement provided the lowest cost configuration because the capital cost required to add more photovoltaics is greater than the capital cost reduction associated with fewer electrolyzer units. A basic calculation that demonstrates this follows. The base-case photovoltaic area per electrolyzer stack is $7.6 \times 10^4 m^2/stack$. In the limit of removing a single electrolyzer stack (500 kg H_2 /day capacity), one would need $\sim 7.6 \times 10^4 m^2$ of additional photovoltaic area, which would be an additional \$3.9 MM of capital (base-case values), while the removal of a single electrolyzer stack would result in a \$0.98 MM reduction in capital. Thus, the capital cost of the additional photovoltaic arrays outweighs that of the electrolysis units. This simple analysis does not consider the value of the extra electricity produced by the additional photovoltaic area that could be sold to the grid and/or used onsite.

Capacity Factor

The maximum capacity factor values were calculated based on hourly radiant energy density data for each month from 2005-2010 for Daggett, CA⁶. The global tilted radiant energy density data was used for all systems except the Type 4 system, which used the direct tilted radiant energy density data calculated from the direct normal radiant energy density data available. Equation 1 was used to calculate the capacity factor where each monthly averaged hourly radiant energy density profile was multiplied by the number of days in that month and summed for all hours in that month and months in that year to obtain the maximum amount of solar power that could possibly be absorbed per m^2 . This value was divided by the peak irradiance summed over all wavelengths ($1000 W\cdot m^{-2}$) and the number of hours in a year.

$$Capacity\ Factor_{year} = \frac{\sum_{j=1}^{12\ Months} \sum_{i=1}^{24\ hrs} Radiant\ energy\ density_{hr,month} \left(\frac{W-hr}{m^2} \right) * DPM \left(\frac{day}{month} \right)}{\left(1000 \frac{W}{m^2} \right) \left(8760 \frac{hrs}{year} \right)} \quad (1)$$

The direct tilted radiant energy density for the Type 4 system was calculated assuming 100% collection of all direct incident light, though this is unlikely because of the lack of tracking for the 10x concentrator system⁷. The direct normal radiant energy data were adjusted based on the solar azimuthal and zenith angles to obtain the direct tilted radiant energy density based on Equations 2 and 3 (collected from ref. ⁸ for 34N, 116W and GTM offset = -7 hrs on the 15th of each month). Here, θ is the tilt angle (set to the latitude, 34°), θ_z is the solar zenith angle, β is the panel tilt angle, γ_s is the solar azimuth angle and γ is the panel azimuth angle (set to 180° for optimal solar collection in the northern hemisphere).

$$DTI = \cos(\theta) DNI \quad (2)$$

$$\cos(\theta) = \cos(\theta_z) \cos(\beta) + \sin(\theta_z) \sin(\beta) \cos(\gamma_s - \gamma) \quad (3)$$

The base-case capacity factor for the Type 4 system was calculated based on the ratio of the maximum operating factors and the base-case operating factor for the

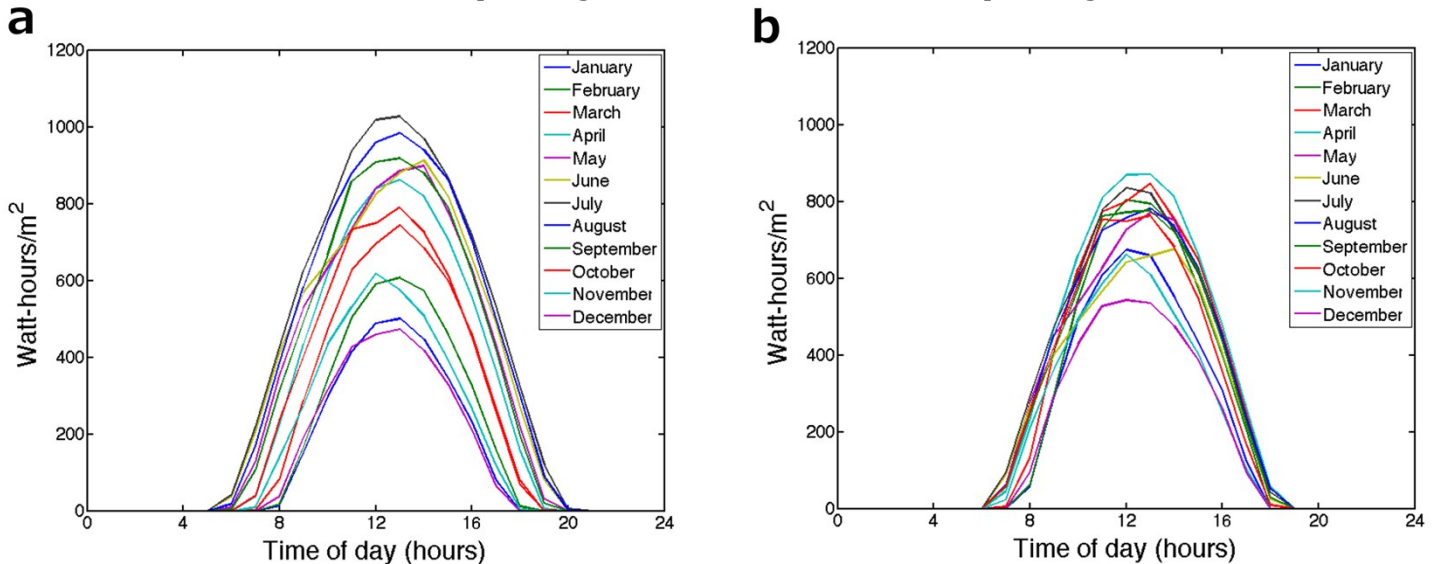


Figure S 1: Radiant energy density versus the time of day for (a) global tilted solar irradiation and (b) direct tilted solar irradiation

The value used for the base-case of the non-concentrated systems is different than other recently reported AC capacity factors for photovoltaics in the southwestern U.S.⁹. The photovoltaic AC capacity factor is equivalent to the capacity factor used in this study because it does not include AC-DC conversion losses and thus is higher than DC capacity factors. As indicated in ref. ⁹ the high AC capacity factors for photovoltaic installations are due to an oversizing of the installed photovoltaic capacity as compared to the inverter capacity. Because the capacity rating is based on the inverter capacities in these systems, the oversized photovoltaic array artificially makes the capacity factor higher than physically possible based on integration of the solar resource in those regions.

Financial Calculations

Many cost estimates for system components were taken from reports/quotes in the past. These were future valued to 2014 \$ by Equation 5 using an inflation rate of 1.9%.

$$Future\ Value(2014\ \$) = Reported\ Value\ (\#\#\#\ \$)(1 + 0.019)^{2014 - \#\#\#} \quad (5)$$

Solar Area Calculations

The area required for the solar absorbing component of the system was calculated based on the following equation.

$$Area\ (m^2) = \frac{10000 \left(\frac{kg\ H_2}{day} \right) 1.2 \times 10^8 \left(\frac{J}{kg\ H_2} \right)}{1000 \left(\frac{W_p}{m^2} \right) \eta_{STH} 3600 \left(\frac{s}{hr} \right) 24 \left(\frac{hr}{day} \right) ofac_{solar}} \quad (6)$$

Number of PEM Electrolyzer Stack Calculations

$$Number\ of\ Stacks = \frac{10000 \left(\frac{kg\ H_2}{day} \right)}{500 \left(\frac{kg\ H_2}{stack} \right) of\ ac_{electrolzer}} \quad (7)$$

Discussion Calculations

Carbon Tax

To calculate the carbon tax (\$ kg⁻¹ H₂) for the base-case Type 3 and 4 PEC systems, Equation 9 was used with the SMR CO₂ intensity taken from industrial data.¹⁰ The target systems were assumed to have a CO₂ intensity of zero.

$$Carbon\ Tax \left(\frac{\$}{t\ CO_2} \right) = \frac{Target\ System \left(\frac{\$}{kg\ H_2} \right) - SMR \left(\frac{\$}{kg\ H_2} \right)}{SMR\ CO_2\ Intensity \left(\frac{t\ CO_2}{kg\ H_2} \right)} \quad (8)$$

The CO₂ intensity of grid electrolysis was calculated from the total CO₂ associated with electricity generation¹¹ and the total electricity produced¹² in the U.S in 2012 , in conjunction with an electrolysis efficiency of 66% (50 kWh/kg H₂)¹⁰.

CO₂ Electrochemical Reduction Product CO₂ Cost Equivalence

The CO₂ cost equivalence for a variety of known CO₂ electrochemical reduction products on Cu was calculated by first determining the current market value in \$/ton product.¹³ A mass change fraction was then calculated for each product based on the carbon and oxygen content retained from CO₂ in the product molecule. The CO₂ equivalence value is then given by multiplying the product market value by the mass fraction value. This calculation, Equation 9, assumes 100% utilization of CO₂.

$$\begin{aligned}
 & CO_2 \text{ Equivalence} \left(\frac{\$}{\text{ton } CO_2} \right) \\
 &= \text{Product Value} \left(\frac{\$}{\text{ton}} \right) \times \frac{\# \text{ of C in product} \times 12 \left(\frac{g}{\text{mol}} \right) + \# \text{ of O in product} \times 16 \left(\frac{g}{\text{mol}} \right)}{\# \text{ of C in product} \times 44 \left(\frac{g}{\text{mol}} \right)}
 \end{aligned}$$

CO₂ Mass Transport Limitations

Liquid phase mass transport of CO₂ to a submersed electrode surface can limit the maximum achievable rate of reaction. The aqueous mass transport limited flux of CO₂ into the liquid is $\sim 10^{-6}$ mol m⁻² s⁻¹.¹⁴ The equivalent current density is dependent on the number of electrons used per CO₂ in the reduction process, $\# \text{ of electrons per } CO_2 \text{ molecule} \times 10^{-2}$ mA cm⁻². Assuming an 8 electron reduction of CO₂ gives a limiting current density of $\sim 10^{-1}$ mA cm⁻², which is approximately 3 orders of magnitude lower than the limiting current density for a tandem junction cell.

References

- 1 B. D. James, G. N. Baum, J. Perez and K. N. Baum, *Technoeconomic Analysis of Photoelectrochemical (PEC) Hydrogen Production*, Directed Technologies Inc., 2009.
- 2 B. A. Pinaud, J. D. Benck, L. C. Seitz, A. J. Forman, Z. Chen, T. G. Deutsch, B. D. James, K. N. Baum, G. N. Baum, S. Ardo, H. Wang, E. Miller and T. F. Jaramillo, *Energy & Environmental Science*, 2013, **6**, 1983–2002.
- 3 L. A. Zook and J. Leddy, *Analytical chemistry*, 1996, **68**, 3793–3796.
- 4 Y. Chen, C. Xiang, S. Hu and N. S. Lewis, *J Electrochem Soc*, 2014, **161**, F1101–F1110.
- 5 C. Turchi, *Parabolic Trough Reference Plant for Cost Modeling with the Solar Advisor Model (SAM)*, National Renewable Energy Laboratory, 2010.
- 6 *National Solar Radiation Data Base*, National Renewable Energy Laboratory.
- 7 R. Winston, J. C. Minano and P. Benitez, *Nonimaging Optics*, Elsevier Academic Press, 2005.
- 8 C. Honsberg and S. Bowden, Eds., *Sun Position Calculator*.
- 9 M. Bolinger and S. Weaver, *Utility-Scale Solar 2012*, Lawrence Berkeley National Laboratory, 2013.
- 10 D. Bonaquist, *Analysis of CO₂ Emissions, Reductions, and Capture for Large-Scale Hydrogen Production Plants*, Praxair, 2010.
- 11 *How much of U.S. carbon dioxide emissions are associated with electricity generation?* U.S. Energy Information Administration.
- 12 *Electricity Data Browser*, U.S. Energy Information Administration.
- 13 K. P. Kuhl, E. R. Cave, D. N. Abram and T. F. Jaramillo, *Energy & Environmental Science*, 2012, **5**, 7050.
- 14 H. Herzog, *Assessing the Feasibility of Capturing CO₂ from the Air*, MIT Laboratory for Energy and the Environment, 2003.